Materials Research Proceedings 33 (2023) 369-375 https://doi.org/10.21741/9781644902677-54

Simulation of flow field characteristics in gap between high-speed rocket sled slipper and track

Tianjiao Dang [1,2,a], Zhen Liu [1,b,*], Pierangelo Masarati [2,c]

[1]State Key Laboratory for Strength and Vibration of Mechanical Structures, Xi'an Jiaotong University, Xi'an, Shaanxi, 710049, P.R. China

[2]Department of Aerospace Science and Technology, Politecnico di Milano, via La Masa 34, Milano, 20156, Italy

[a] tianjiao.dang@polimi.it, [b,*] liuz@mail.xjtu.edu.cn, [c] pierangelo.masarati@polimi.it

Keywords: Gap Flow Field, Computational Fluid Dynamics, Aerodynamics, Supersonic

Abstract. Accurate simulation of flow field characteristics within the gap between the slipper and track is essential for the prevention of aerodynamic heat damage to high-speed rocket sleds. A three-dimensional structured mesh was utilized to establish the flow field model in the slipper-track gap, while computational fluid dynamics was employed for simulating the flow field movement. The results revealed that the bow shock wave at the head of the rocket sled has a significant influence on the flow field characteristics within the gap. Specifically, the velocity of the mainstream in the gap initially exhibited an increasing trend, followed by a decreasing trend, and then a re-increase. Conversely, the mainstream temperature displayed a decreasing trend initially, followed by an increasing trend, and then a decrease once more. The air compression within the slipper-track gap resulted in remarkably high temperatures, with the maximum temperature reaching 1160 K at Ma = 4 in the immediate vicinity of the slipper. The current investigation provides valuable insights that can guide future research on the structural characteristics of slippers in high-temperature environments.

Introduction

The high-speed rocket sled is a remarkable and precise piece of ground testing equipment that was developed in the mid to late 20th century. It can solve a range of performance test issues encountered during aircraft aerodynamic experiments in high-speed and high-load environments [1-4]. In contrast to wind tunnel tests that employ scaled-down models, the rocket sled is tested using a full-scale model of the aircraft. It is extensively employed in the aviation, aerospace, and defense industries to research and develop a variety of products, such as aviation lifesaving seat ejection tests, missile guidance, and aircraft rain erosion. During the test, the rocket engine propels the sled along the track at high speed, while the test product's performance parameters affixed to the sled are measured with precision.

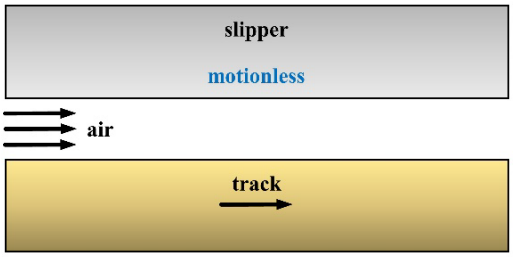

Fig. 1. Gap between slipper and track

Content from this work may be used under the terms of the Creative Commons Attribution 3.0 license. Any further distribution of this work must maintain attribution to the author(s) and the title of the work, journal citation and DOI. Published under license by Materials Research Forum LLC.

Materials Research Proceedings 33 (2023) 369-375 https://doi.org/10.21741/9781644902677-54

The *slipper* is a crucial component of the rocket sled that makes contacts with the track, preventing the sled from flying off during movement. During the design phase, a narrow gap is intentionally left between the slipper and the track to avoid it getting stuck during operation. However, due to the high speed of the slipper and the stationary nature of the track, there exists a significant velocity difference between the upper and lower surfaces of the gap, as illustrated in Fig. 1. This results in a high-gradient flow field within the gap, which can generate extreme temperatures. Such high-speed and high-gradient flow fields can cause damage to the slipper and alter its material properties. Thus, it is crucial to accurately simulate the flow field characteristics in the gap to ensure the thermal protection of the rocket sled slipper.

Two main methods, theoretical analysis and numerical simulation, have been employed to investigate the characteristics of the high-speed rocket sled slipper-track gap flow field. Notably, Korkegi and Briggs [5] have made significant contributions to the study of slipper-track gap flow. Given the high velocity of fluid in the slipper-track gap of high-speed rocket sleds, the fluid is compressible. The authors [6] identified the presence of compressible turbulence in the gap and developed a theoretical model to derive the velocity and temperature curves of two-dimensional compressible flow. When the fluid flows close to a solid surface, the velocity of the fluid decreases due to drag, resulting in the formation of a boundary layer. The authors [7] argued that supersonic flow entering the initial stage of the gap would create shock waves, followed by the formation of boundary layers on the surface of both the slipper and the track. These two boundary layers converge at a specific point within the gap, as deduced by the authors. In a subsequent paper, the same authors [8] demonstrated that a decrease in gap height results in a corresponding pressure decrease, and vice versa.

With the increase in computer processing speed, computational fluid dynamics (CFD) method was applied to the numerical simulation of the slipper-track gap flow field of high-speed rocket sled. The Air Force Institute of Technology (AFIT) at the Air University in the United States has conducted extensive research in this field. Lofthouse [9] utilized the CFD method to compute the three-dimensional steady inviscid flow field of the slipper-track gap of high-speed rocket sleds at varying speeds, thereby predicting the pressure gradient within the narrow gap. However, the accuracy of the results was limited to first order due to the use of an unstructured mesh. Moreover, since the flow field was assumed to be inviscid, the temperature within the narrow gap could not be accurately calculated, although its influence on pressure calculation was minimal. Alban [10] conducted a comprehensive investigation of the aerodynamic heating within the slipper-track gap and improved the accuracy of temperature predictions using a one-dimensional finite difference model. Subsequently, Alban replaced the one-dimensional finite difference model with a two-dimensional finite element model to simulate the temperature distribution within the gap with greater precision.

The study of the flow field in the slipper-track gap of high-speed rocket sled has made significant progress, yet there is still much room for improvement. The current studies have shown high accuracy in one and two dimensions but have used an unstructured mesh in the three-dimensional model, leading to reduced computational accuracy. To address this issue, this study seeks to enhance the accuracy of the three-dimensional model using a structured mesh. This will enable a more precise calculation of the flow field in the slipper-track gap of high-speed rocket sled and allow for exploration of the movement of the flow field within the gap. Ultimately, the results of this study will provide a foundation for further research on heat transfer in the slipper-track gap.

This paper is organized as follows: Section 1 provides an overview of the study's background, significance, and current status. Section 2 outlines the theoretical framework and modeling approach. Section 3 presents the calculation results and analysis. Finally, Section 4 summarizes the key findings and conclusions.

Materials Research Proceedings 33 (2023) 369-375 https://doi.org/10.21741/9781644902677-54

Methods

In this study, the numerical method was utilized to calculate the flow field in the slipper-track gap of high-speed rocket sled. The finite volume method was employed to solve the three-dimensional steady compressible Navier-Stokes equations. The governing equation is expressed as

$$\frac{d}{dt}\iiint Q d\Omega + \oiint \vec{H}^I \cdot \vec{n} dS = \oiint \vec{H}^V \cdot \vec{n} dS, \quad (1)$$

where Q is the state variable, including the density, momentum component, and total energy of the fluid. $\vec{H}^I$ is the inviscid flux vector on the boundary surface of the control body, $\vec{H}^V$ is the viscous flux vector, Ω is the volume of the control body, S is the area of the boundary surface of the control body, and $\vec{n}$ is the normal vector of the boundary surface.

The solution format and turbulence model are critical factors that can significantly impact the accuracy of numerical calculations. To minimize the impact of non-physical dissipation on accuracy, inviscid fluxes are discretized using Roe's Flux Difference Splitting scheme [11], and the entropy method was used to correct non-physical solutions. The Roe format has proven to be one of the most effective formats in practical applications due to its exceptional ability to resolve viscous and shock wave discontinuities. For the spatial discretization, the second-order upwind scheme was utilized. In this study, the two-equation $k-\omega$ SST turbulence model was employed to calculate turbulence. This model combines the advantages of $k-\varepsilon$ model and $k-\omega$ model. The equations of this model are

$$\frac{\partial}{\partial t}(\rho k) + \frac{\partial}{\partial x_j}(\rho k u_j) = \frac{\partial}{\partial x_j}\left[\left(\mu + \frac{\mu_t}{\sigma_k}\right)\frac{\partial k}{\partial x_j}\right] + G_k - Y_k + S_k \quad (2)$$

and

$$\frac{\partial}{\partial t}(\rho \omega) + \frac{\partial}{\partial x_j}(\rho \omega u_j) = \frac{\partial}{\partial x_j}\left[\left(\mu + \frac{\mu_t}{\sigma_\omega}\right)\frac{\partial \omega}{\partial x_j}\right] + G_\omega - Y_\omega + D_\omega + S_k, \quad (3)$$

where G_k and G_ω are the generation terms of k and ω. Y_k and Y_ω are the dissipation terms of k and ω. D_ω is the cross-diffusion term, and S_k is the self-defined source term.

In this study, a three-dimensional model of the rocket sled and track was developed to investigate the flow field in the slipper-track gap. The model consisted of a rocket sled, a slipper, and a track, with a narrow gap between the slipper and track. To numerically solve the flow field, the finite volume method was employed and the domain was discretized into a structured mesh, as illustrated in Fig. 2. The discretization of the mesh and calculation were based on the commercial software ANSYS ICEM CFD [12] and Fluent [13], respectively. The resulting cell number was approximately 9 million. In the areas where the flow field parameters vary greatly, such as the sled head, windward side of the slipper, and boundary layer, a denser grid was employed to better capture the characteristics of the flow field near the structure surface.

The flow field was set as a cuboid. The inlet and far field of the flow field were set as far-field boundaries; the outlet was set as a supersonic outlet boundary; the sled and the slipper were set as non-slip adiabatic walls. The track and the ground were set as translational walls, whose translational speed was consistent with the incoming flow speed. A free incoming flow static pressure p_0 = 101,325 Pa and static temperature T_0 = 288.15 K were defined. Sea level pressure and temperature parameters were used, and the ideal gas model was applied. The slipper-track gap flow field characteristics of the rocket sled at Mach numbers of 2 and 4 were computed. After 25,000 steps, the residual curve converged below 10^{-4} to reach the steady state

Materials Research Proceedings 33 (2023) 369-375 https://doi.org/10.21741/9781644902677-54

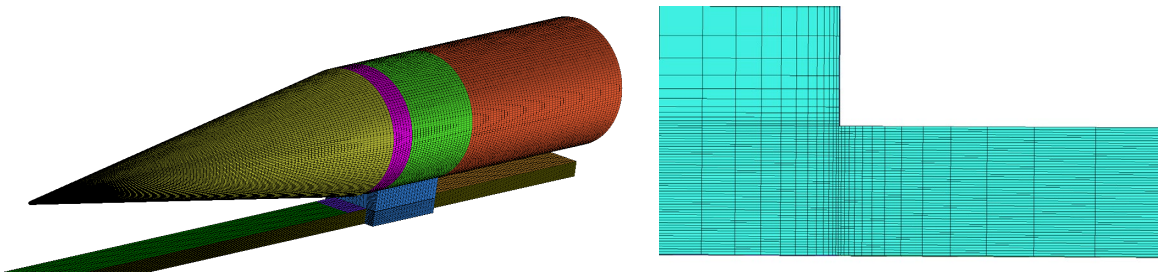

(a) Grids on the surface of the structure (b) Grids in the slipper-track gap

Fig. 2. Structured mesh of the flow field

Results and discussion

Fig. 3 illustrates the pressure distribution at *Ma* = 2. The figure showcases several features of the flow field that merit discussion. Specifically, Fig. 3(a) reveals the formation of bow shock waves at the fore of the rocket sled. These bow shock waves are comprised of a central normal shock wave, surrounded by oblique shock waves on either side. Fig. 3(b) further highlights the emergence of an annular high-pressure region at the outlet of the flow field and on the ground. Furthermore, the slipper-track gap flow field characteristics are influenced by the shock wave reflecting off the track and the ground. Finally, Fig. 3(c) also indicates the presence of a distinct normal shock wave at the gap's entrance, which is consistent with the theory advanced in Reference [7].

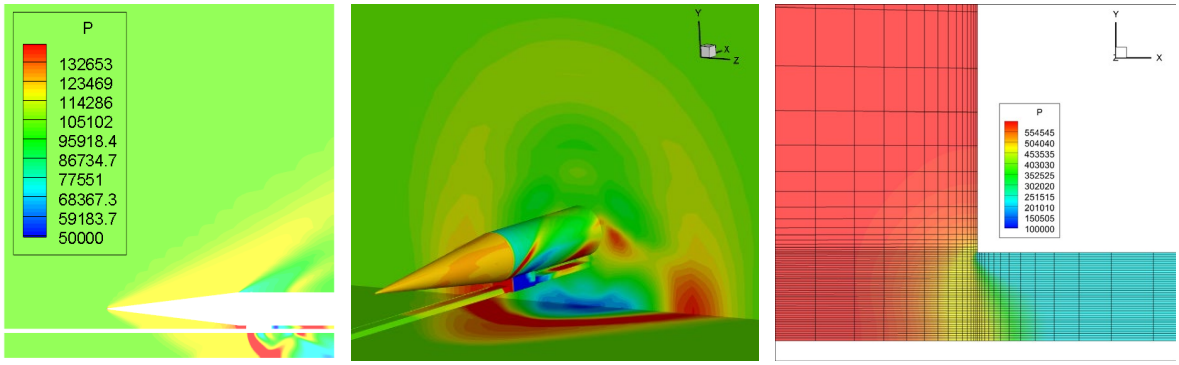

(a) Cross section (b) Axonometric projection (c) Slipper-track gap

Fig. 3. Pressure distribution at Ma = 2

In this study, we analyzed the flow field at *Ma* = 4 with the aim of determining the distribution of physical quantities and the variation rules within the slipper-track gap. To achieve this objective, we selected ten observation points along the X-axis of the gap, as illustrated in Fig. 4. Observation point 1 is located at the leading edge of the gap, while observation point 10 is situated at the trailing edge. To account for the significant variation of the flow field at the leading and trailing edges and the comparatively small variation in the middle section, we adopted a dense-sparse-dense distribution mode for the observation points.

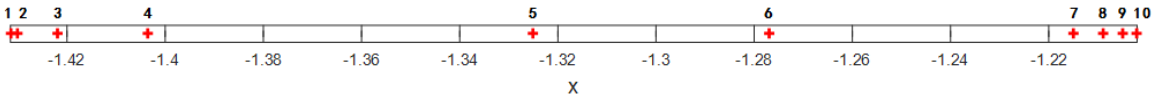

Fig. 4. Observation points at the slipper-track gap

In Fig. 5, we present the physical quantity profiles at different locations within the slipper-track gap at *Ma* = 4. Fig. 5(a) shows the velocity profiles at ten observation points. The velocity curves exhibit a similar trend along the gap flow direction. At the gap inlet, the mainstream velocity is about 600 m/s. Subsequently, the velocity gradually increases from the inlet to the stable section before slightly decreasing again. Upon reaching the stable stage, the velocity near the upper and lower walls rises due to the increase in fluid viscosity, while the mainstream velocity slightly

Materials Research Proceedings 33 (2023) 369-375 https://doi.org/10.21741/9781644902677-54

decreases. At the outlet section, the mainstream velocity experiences a sharp increase, reaching approximately 900 m/s. Fig. 5(b) presents the temperature profiles of ten observation points. At the gap inlet, there is a high-temperature zone in the upper region, whereas the temperature near the lower wall is lower. While the temperature in the inlet section remains consistent in shape, it slightly decreases. The temperature then increases from the inlet section to the stable section. The temperature profile gradually transitions to a lower temperature in the mainstream area and a higher temperature at the upper and lower walls, with the temperature gradient near the lower wall being zero. The temperature profile in the stable stage remains constant, with the mainstream temperature slightly increasing to 1110 K. In the outlet section, the temperature experiences a significant decrease, with the upper part of the gap outlet being a low-temperature zone and the temperature near the lower wall being higher. The mainstream temperature at the outlet is approximately 870 K. To summarize, the narrow gap's temperature is exceptionally high, which could modify the slipper's material properties.

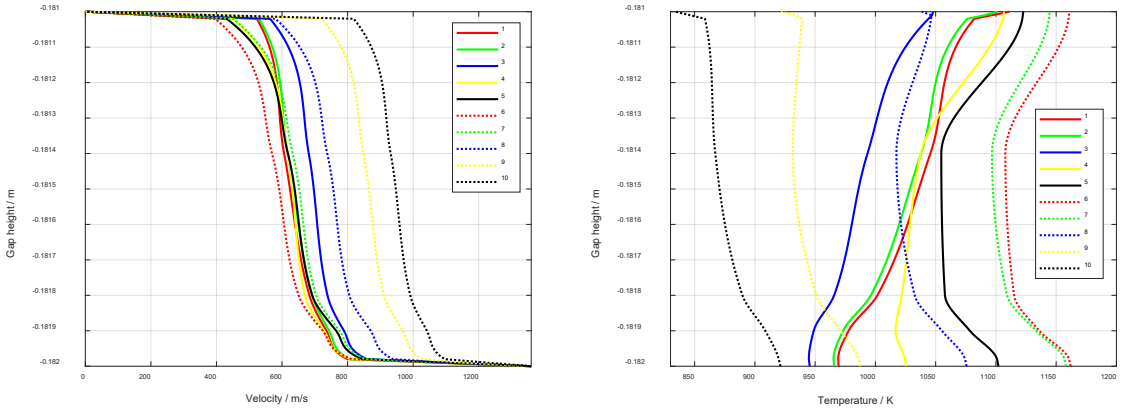

(a) Velocity profiles (b) Temperature profiles

(c) Density profiles

Fig. 5. Physical quantity profiles at different positions in the gap

In Fig. 5(c), we present the density profiles of ten observation points at Ma = 4. The compression effect is more pronounced in the lower part of the fluid near the gap inlet. Therefore, the air density in the inlet area increases from the upper wall to the lower wall. The density profile retains the same shape, but there is a slight decrease. As one moves from the inlet section to the stable section, the density increases, and the mainstream density reaches 13 kg/m^3. The density profile gradually shifts such that the mainstream density is higher, while the density near the upper and lower walls is lower. The density profile remains constant until the outlet section, where there

is an abrupt drop in density, and the mainstream density is about 7.5 kg/m^3. Thus, the high air density in the narrow gap suggests significant air compression.

Conclusions

The high-speed rocket sled is a crucial tool in the aviation and aerospace. This study utilized a three-dimensional structured mesh to establish a relatively accurate model of the flow field in the slipper-track gap of a high-speed rocket sled. The simulation provided insight into the movement law of the flow field within the gap.

At Ma = 2, the pressure distribution within the gap revealed that the bow shock wave at the head of the rocket sled impacted the flow field characteristics. Moreover, an obvious normal shock wave was detected at the entrance of the gap. At Ma = 4, the shapes of velocity curves along the gap flow direction were nearly identical. Initially, the mainstream velocity increased, then decreased, and finally increased again. In contrast, the mainstream temperature first decreased, then increased, and eventually decreased once more. The temperature near the upper wall of the gap inlet was higher, whereas the temperature at the lower part of the outlet was elevated. The air density of the lower portion at the gap inlet was the largest, and it gradually became the largest in the mainstream area.

In conclusion, the air in the slipper-track gap undergoes significant compression, resulting in very high temperatures. At Ma = 4, the highest temperature near the slipper can reach 1160 K, which poses a potential risk of damage to the slipper. This study provides a foundation for further research on the structural characteristics of slippers in high-temperature environments.

Acknowledgments

The first author acknowledges the financial support by the China Scholarship Council (No. 202106280004).

References

[1] Dang T, Liu Z, and Zhou X, et al, Dynamic response of a hypersonic rocket sled considering friction and wear, Journal of Spacecraft and Rockets. 59 (2022) 1289-1303. https://doi.org/10.2514/1.A35267

[2] Cinnamon John D., and Anthony N. Palazotto, Analysis and simulation of hypervelocity gouging impacts for a high speed sled test, International Journal of Impact Engineering. 36 (2009) 254-262. https://doi.org/10.1016/j.ijimpeng.2007.11.009

[3] Dang T, Li B, and Hu D, et al, Aerodynamic design optimization of a hypersonic rocket sled deflector using the free-form deformation technique, Proceedings of the Institution of Mechanical Engineers, Part G: Journal of Aerospace Engineering. 235 (2021) 2240-2248. https://doi.org/10.1177/09544100221075071

[4] Szmerekovsky Andrew G., and Anthony N. Palazotto, Structural dynamic considerations for a hydrocode analysis of hypervelocity test sled impacts, AIAA Journal. 44 (2006) 1350-1359. https://doi.org/10.2514/1.13803

[5] Korkegi Robert H., and Ronald A. Briggs, On compressible turbulent-plane Couette flow, AIAA Journal. 6 (1968) 742-744. https://doi.org/10.2514/3.4583

[6] Korkegi Robert H., and Ronald A. Briggs, Compressible turbulent plane Couette flow with variable wall temperature, Aerospace research labs Wright-Patterson AFB Ohio, 1970. https://apps.dtic.mil/sti/citations/AD0708162

[7] Korkegi Robert H., and Ronald A. Briggs, The hypersonic slipper bearing-A test track problem, Journal of Spacecraft and Rockets. 6 (1969) 210-212. https://doi.org/10.2514/3.29570

[8] Korkegi R. H., and R. A. Briggs, Compressible turbulent plane Couette flow with variable heat transfer based on von Karman model, AIAA Journal. 8 (1970) 817-819. https://doi.org/10.2514/3.5767

[9] Lofthouse A., M. Hughson, and A. Palazotto, Hypersonic test sled external flow field investigation using computational fluid dynamics, 40th AIAA Aerospace Sciences Meeting & Exhibit, 2002. https://doi.org/10.2514/6.2002-306

[10] Alban Christopher J, Thermal and melt wear characterization of materials in sliding contact at high speed, Air Force Institute of Technology, Wright-Patterson AFB Ohio, Graduate school of engineering and management, 2014. https://apps.dtic.mil/sti/citations/ADA599170

[11] Roe Philip L, Approximate Riemann solvers, parameter vectors, and difference schemes, Journal of computational physics. 43 (1981) 357-372. https://doi.org/10.1016/0021-9991(81)90128-5

[12] Ansys® ICEM CFD, Release 2020 R1, help system, ANSYS, Inc.

[13] Ansys® Fluent, Release 2020 R1, help system, ANSYS, Inc.